Materials Science and Engineering C 33 (2013) 2229–2234

Contents lists available at SciVerse ScienceDirect

Materials Science and Engineering C

journal homepage: www.elsevier.com/locate/msec

Label-free detection of aflatoxin M1 with electrochemical Fe_3O_4/polyaniline-based aptasensor

Binh Hai Nguyen [a,1], Lam Dai Tran [a,*,1], Quan Phuc Do [b], Huy Le Nguyen [c], Ngoc Huan Tran [d], Phuc Xuan Nguyen [a]

[a] Institute of Material Science, Vietnam Academy of Science and Technology, 18, Hoang Quoc Viet Road, Cau Giay, Hanoi, Viet Nam
[b] Research Center for Environmental Technology and Sustainable Development, Hanoi University of Science, Hanoi, Viet Nam
[c] School of Chemical Engineering, Hanoi University of Science and Technology, 1, Dai Co Viet Road, Hanoi, Viet Nam
[d] Department of Chemistry, Hanyang University, Seoul 133-791, Republic of Korea

ARTICLE INFO

Article history:
Received 6 August 2012
Received in revised form 13 December 2012
Accepted 19 January 2013
Available online 28 January 2013

Keywords:
Fe_3O_4-doped polyaniline
Aptasensor
Aflatoxin M1 (AFM1)
Electrochemical detection

ABSTRACT

The selective detection of ultratrace amounts of aflatoxin M1 (AFM1) is extremely important for food safety since it is the most toxic mycotoxin class that is allowed to be present on cow milk with strictly low regulatory levels. In this work, Fe_3O_4 incorporated polyaniline (Fe_3O_4/PANi) film has been polymerized on interdigitated electrode (IDE) as sensitive film for AFM1 electrochemical biosensor. The immobilized aptamers as an affinity capture reagent and magnetic nanoparticles for signal amplification element have been employed in the sensing platform. Label-free and direct detection of the aptamer-AFM1 on Fe_3O_4/PANi interface were performed via electrochemical signal change, acquired by cyclic and square wave voltammetries. With a simplified strategy, this electrochemical aptasensor shows a good sensitivity to AFM1 in the range of 6–60 ng·L^{-1}, with the detection limit of 1.98 ng·L^{-1}. The results open up the path for designing cost effective aptasensors for other biomedical applications.

1. Introduction

Extremely serious human health disorders such as hepatocellular carcinoma, aflatoxicosis, Reye's syndrome and chronic hepatitis are proved to be caused by the aflatoxins (AFs), which is a group of toxic metabolites, consisting of a coumarin and a double furan ring. The AFs are also a major class of mycotoxins that are mainly produced by a variety of molds such as *Aspergillus flavus* and *Aspergillus parasiticus* [1–4]. AFs are carcinogenic and present in grains, nuts, cottonseed and other commodities associated with human food or animal feeds. Among the four most important sub-types, AFB1, AFB2, AFG1 and AFG2, AFB1 is the most toxic form due to their "double-hazardous" effect to both DNA and proteins. As was mentioned in the previous research, the toxicity of AFB1 is 10, 68, and 416 times higher than that of KCN, arsenic and melamine, respectively [5]. When cows are fed with contaminated foodstuff, AFB1 is converted by hydroxylation to AFM1 with the help of the liver enzyme cytochrome P450, which is subsequently secreted in the milk of lactating cows. AFM1 (Fig. 1) is quite stable towards the normal milk processing methods such as pasteurization and if present in raw milk, it may still persist into the final products for human consumption. Numerous countries have declared limits for the presence of AFM1 in milk products. In the European Union countries the limit for the presence of AFM1 in milk and reconstituted milk powders has been set at 50 ng·L^{-1} or 50 parts per trillion (50 ppt).

Usually, AFM1 analysis is performed by ELISA (enzyme-linked immunosorbent assay) [6–14], TLC (thin layer chromatography) [15–18] and HPLC (high-performance liquid chromatography) [19–21]. On the other hand, an immunosensor array of 96 screen-printed electrode coupled with a multichannel electrochemical detection (MED) system using the intermittent pulse amperometry (IPA) technique has been also used for the detection of AFM1 and AFB1 [22,23]. However, the selectivity, sensitivity as well as the operation simplicity are still major technical challenges of the above analytical methods.

Meanwhile, electrochemical biosensor in general and aptasensor (based on highly specific molecular recognition of antigens by aptamer) in particular, have received considerable attention regarding the detection of various biomolecules owing to the advantages of low cost, simplicity, high sensitivity, compatibility with mass manufacturing and possibility of microfabrication, thus making them excellent candidates for many point-of-care (portable) diagnostics/detections, including AFM1. Reported for the first time in 1990 [24,25], aptamer (APT), functional short oligonucleotides, selected from combinatorial libraries through *in vitro* selection, can bind with high affinity and specificity to a wide range of target molecules, such as drugs, proteins, toxins or other organic or inorganic molecules [26–28]. In contrast to production of the antibodies, which involve *in vivo* immunization of animals, aptamers can be generated by an *in vitro* selection process

* Corresponding author. Tel.: +84 4 37564129; fax: +84 438360705.
E-mail address: lamtd@ims.vast.ac.vn (L.D. Tran).
[1] These authors equally contributed to this paper.

0928-4931/$ – see front matter © 2013 Elsevier B.V. All rights reserved.
http://dx.doi.org/10.1016/j.msec.2013.01.044

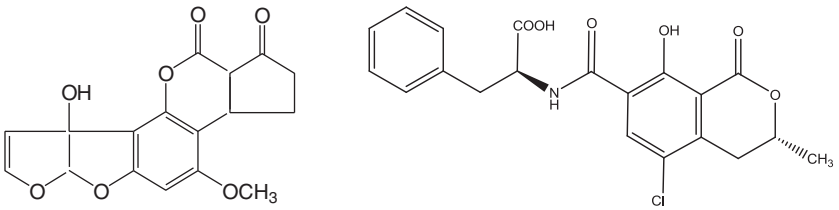

Aflatoxin M1(AFM1) Ochratoxin A (OTA)

Fig. 1. Aflatoxin M1 (AFM1) and ochratoxin A (OTA).

called SELEX (Systematic Evolution of Ligands by EXponential enrichment), obviating the use of animals [24,25]. Being produced easily and reproducibly at large scale, by chemical synthesis (that explains why APT also called as chemical antibodies), APTs are known to be cost-effective and enough stable in terms of temperature and biological activity, with dissociation constants comparable to most of the monoclonal antibodies [29]. Briefly, the interest in APTs originates from their important advantages over antibodies such as easier *in vitro* production, smaller size (molecular mass 5–15 kDa), thus allowing a greater surface density of receptors and consequently, more important specificity [29–31].

Numerous studies have been also reported on the development of aptasensors, based on different signal transducers. Particularly, the detection of AFM1 has been reported by direct competitive assay using a peroxidase-aptamer tracer as the enzymatic label. With the use of this approach, the detection limit for AFM1 in milk was reported to be 8 $ng \cdot L^{-1}$, in a dynamic detection range of 10–100 $ng \cdot L^{-1}$, which meets the present legislative limits of 50 $ng \cdot L^{-1}$ [32].

The objective of this work is to further improve the sensitivity for AFM1 analysis, by using controlled covalent immobilization of aptamers on −COOH functionalized superparamagnetic nanoparticles. Magnetic nanoparticles (MNPs) are expected to greatly improve the kinetics of immunoreactions as well as increase the binding site for biochemical reaction between the reagent (aptamer, APT) and samples (AFM1). In addition, conducting PANi based interface can also contribute to enhancing the conductivity and thus sensitivity of sensor.

Briefly, this original strategy combines the advantages of the integrated immunoreaction with aptamer and label-free electrochemical transduction between the aptamer, immobilized on MNPs and its specific AFM1, without any label.

2. Experimental

2.1. Chemical and biochemical reagents

Glutaraldehyde was provided by *Sigma*. AFM1, (from *Aspergillus flavus*), ochratoxin A (from *Petromyces albertensis*, ≥98% (TLC) (OTA, used in selectivity experiment), 21-mer aptamer sequence (5′-ACT GCT AGA GAT TTT CCA CAT-3′) was obtained from SELEX procedure and was kindly provided by the Institute of Biotechnology, Vietnam Academy of Science and Technology. Aniline (*Merck*, 99.5%) was distilled under vacuum prior to polymerization. Other chemicals were all of analytical reagent grade without further purification. Aqueous solutions were made with deionized water (18 MΩ).

2.2. Characterization methods

Infra-Red (IR) spectra were recorded with Nicolet 6700 FT-IR Spectrometer, using KBr pellets, in the region of 400–4000 cm^{-1}, with a resolution of 4 cm^{-1}. Field Emission Scanning Electron Microscope (FE-SEM) image was analyzed by Hitachi S-4800. The morphology of Fe_3O_4/PANi composite film on the array was observed by SPM 5100/5500 (Agilent) with PicoPlus 5.3 software. The magnetic properties of Fe_3O_4 nanoparticles were measured with home-made vibrating sample magnetometer (VSM) and evaluated in terms of saturation magnetization (M_s) and coercivity (H_c).

2.3. Sensor fabrication

The interdigitated electrode array (IDA) was fabricated on a silicon substrate via lithography technique. Silicon wafers were covered with a layer of SiO_2 1 μm thick by means of dry oxidation. The wafer was spin-coated with a layer of photoresist AZ5214E (1 μm thickness) and the structure of the electrodes was defined by UV-photolithography. Then, chromium (Cr) and platinum (Pt) layers were sputtered on the top of the wafer with the thickness of 50 and 500 nm, respectively. The working and counter electrodes were patterned by a lift-off process (30 s in acetone solution with ultrasonic vibration). A second photolithographic step is carried out to deposit the silver (Ag) layer. Next, the sensor was immersed into a 0.1 M KCl solution with the Ag and Pt electrodes were connected to the anode and cathode, respectively, of a power supply. A current of 1 mA was applied for 10 s in order to cover the Ag reference electrode with AgCl. The final diameter of the working electrodes was 500 μm. The array, consisting of 12 working electrodes, Ag/AgCl pseudo reference and Pt counter electrodes was then coated with Fe_3O_4/PANi thin film.

2.4. Electropolymerization of Fe_3O_4/PANi film

Functionalized Fe_3O_4 were synthesized by dispersion polymerization with Fe_3O_4 magnetic particle as core and poly(Styrene-co-Acrylic Acid) as shell corresponding to *ex situ* and *in situ* capping method, respectively, as described previously [33]. Afterwards, Fe_3O_4/PANi film was electropolymerized on IDA by using cyclic voltammetry (CV) within the potential range from −0.2 to +0.9 V (vs. Ag/AgCl) with sweep rate of 50 $mV \cdot s^{-1}$, for 20 cycles in a fresh solution containing 0.1 M aniline in 0.5 M H_2SO_4 with 1wt.%. Fe_3O_4 nanoparticles (Fig. 2A). Three peaks, observed at *ca.* +0.2 V, +0.4 V and +0.7 V in the above potential range, were widely characterized as redox processes converting Leucoemeraldine to Emeraldine, Emeraldine to intermediate product, and intermediate product to Pernigraniline forms of PANi respectively. To check whether the obtained PANi film is electroactive and the electron transfer takes place across the polymer chain, a series of cyclic voltammograms was recorded at different scan rates (from 10 to 200 $mV \cdot s^{-1}$) and the respective I_p-v^2 dependence was plotted (figures not shown). The redox peaks on IDA intensify with the increasing scans, confirming that the films were electroactive. The straight line plot of I_p-v^2 reveals the surface-confined process of charge transfer. Furthermore, as seen from Fig. 2B, the magnitude of current response for Fe_3O_4/PANi electrode (solid line) increases in comparison to that of bare PANi electrode (dotted line), indicating that Fe_3O_4 can enhance the current response, thus facilitates the electron transfer within the sensing platform of IDA, compared to that of bare PANi electrode, under the same experimental conditions, regarding the electrode design and PANi platform characteristics. The fact that the oxidation peaks were shifted noticeably towards the higher potentials with the increasing scans, whereas

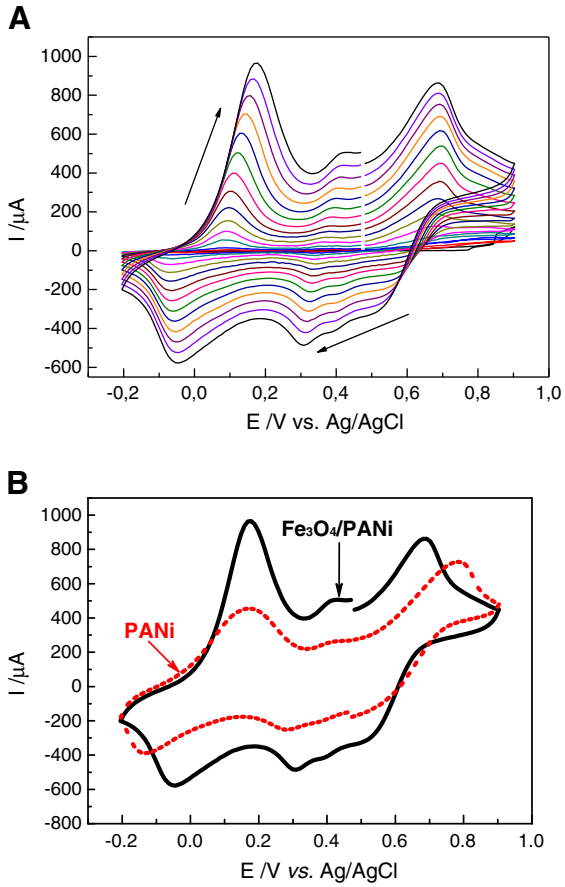

Fig. 2. A. 20 cycles of CVs recorded during Fe_3O_4/PANi composite film growth. B. CV comparison of PANi film (dotted line) with Fe_3O_4/PANi composite (solid line) during electropolymerization.

the reduction peaks moved towards the lower potentials may serve as evidence of Fe_3O_4 role in Fe_3O_4/PANi electrode.

2.5. Aptamer (APT) immobilization and APT–AFM1 reaction conditions

Immobilization of APT onto Fe_3O_4/PANi films has been done using glutaraldehyde as a cross-linker. For immune reaction between APT and its relevant AFM1, APT concentration of 180 pM was used. The electrodes previously grafted with APT were left to react in this solution during 1 h under stirring at 37 °C, and then thoroughly washed in water under stirring at 37 °C. The same immune reaction conditions were applied in selectivity experiment, with irrelevant ochratoxin A (OTA), instead of AFM1.

2.6. Electrochemical measurements

Electrochemical measurements were performed on AUTOLAB PGSTAT 30 (EcoChemie, the Netherlands) under the control of GPES version 4.9. The parameters for CV: scan rate: 50 $mV \cdot s^{-1}$ and potential range of −0.2 to +1.0 V vs. Ag/AgCl. The parameters for SWV were optimized as follows: frequency of 12.5 Hz; start potential of −0.55 V; end potential of +0.25 V; step of 8 mV; and amplitude of 25 mV. Prior to SWV measurements, the electrodes were held for 120 s at the starting potential for conditioning. The SWV scans were repeated until stabilization of the electrochemical signal was completed (*i.e.*, no difference observed between two successive responses). All electrochemical experiments were conducted in 0.1 M HCl at room temperature. Electrochemical detection (SWV and CV) of relevant AFM1 (and irrelevant OTA) was conducted in 0.1 M HCl solution. SWV choice instead of CV is rationalized on its ability to reduce capacitive current as well as the parasite current due to reduction of dissolved oxygen (in SWV, the currents are sampled in both positive and negative pulses successively, furthermore, the registered current is the subtraction between oxidation and reduction currents, thus current density in SWV's is higher than that in CV's recorded for the same electrode [34]).

3. Results and discussion

3.1. APT immobilization and electrochemical detection of APT–AFM1 complexation

Thorough structural and morphological (IR, FE-SEM, AFM, VSM) analyses of Fe_3O_4/PANi electrode surface were provided in Supporting Information (Figs. S1–S4). The whole procedure of aptasensor fabrication was schematically presented in Fig. 3. The immobilization of APT onto the Fe_3O_4/PANi films has been done using crosslinking of glutaraldehyde, which is a dialdehyde capable to form a covalent bond between its aldehyde group and amine group of the other binding molecule. In this case, –CHO of glutaraldehyde reacts in the same time with NH_2 group of PANi chains in the Fe_3O_4/PANi at one end and NH_2 terminus of aminylated APT at the other end, resulting in a stable and robust covalent bonding between them.

The whole procedure of aptasensor fabrication was schematically presented in Fig. 3. In there, ATP was immobilized on the Fe_3O_4/PANi films via glutaraldehyde crosslinking, which is a dialdehyde capable to form a covalent bond between its aldehyde group and amine group of the other binding molecule. In this case, –CHO of glutaraldehyde reacts with NH_2 group of PANi and NH_2 terminus of aminylated APT simultaneously, resulting in a stable sensing layer.

Generally, the definitive principles underlying the optimal concentration of APT are to ensure the following criteria: i) the analyte concentration should fall within the linear range; ii) the electrochemical signals, acquired from immune reaction should be strong enough and relatively well-distributed. In this research, a wide dynamic range (6–60 $ng \cdot L^{-1}$) for AFM1 detection was analyzed. The concentration of APT immobilized on electrode surface was chosen for a stoichiometric APT–AFM1 reaction with 60 $ng \cdot L^{-1}$ of AFM1, it was equivalent to 180 pM of APT. The APT density would warrant an efficient completed immune reaction between APT and AFM1. Effectively, 1 pM will induce negligible SWV signal change after APT–AFM1 reaction, whereas for nanomolar range of APT or higher, a full surface blockage is achieved and subsequent APT–AFM1 complexation cannot be detected by CV/SWV (results not shown). On the basic of the above optimized APT concentration, APT–AFM1 complex formation was clearly visualized by CV and SWV for different concentrations of AFM1. The CV and SWV voltammograms were demonstrated in Figs. 4 and 5 respectively.

It can be logically expected that the presence of the APT–AFM1 complex in the vicinity of the polymer/solution interface strongly influences the switching rate of PANi film. Therefore the current changing could be detected after recognition of the APT–AFM1 interaction, in a direct and label-free detection format. In addition, the current was significantly decreased due to the blocking of AFM1 on charge transfer to the electrode surface, corresponding to different concentrations of AFM1 (curves 4–7, Figs. 4 and 5). The CV measurements were in good agreement with SWV measurements.

To evaluate the analytical performance of sensor, a calibration curve was presented with a series of AFM1 (molecular weight is ~328 Da) concentration ranging from 6 to 78 $ng \cdot L^{-1}$ (~18 to 240 pM AFM1 respectively). As was observed, the signal tends to saturate for the concentrations above 60 $ng \cdot L^{-1}$ (~180 pM) of AFM1, as expected according to the above estimation for APT and AFM1 densities. Assuming a linear behavior at low target concentrations the electrochemical assays showed a sensitivity of 4.77 ± 0.2 $\mu A \cdot ng^{-1} \cdot L$

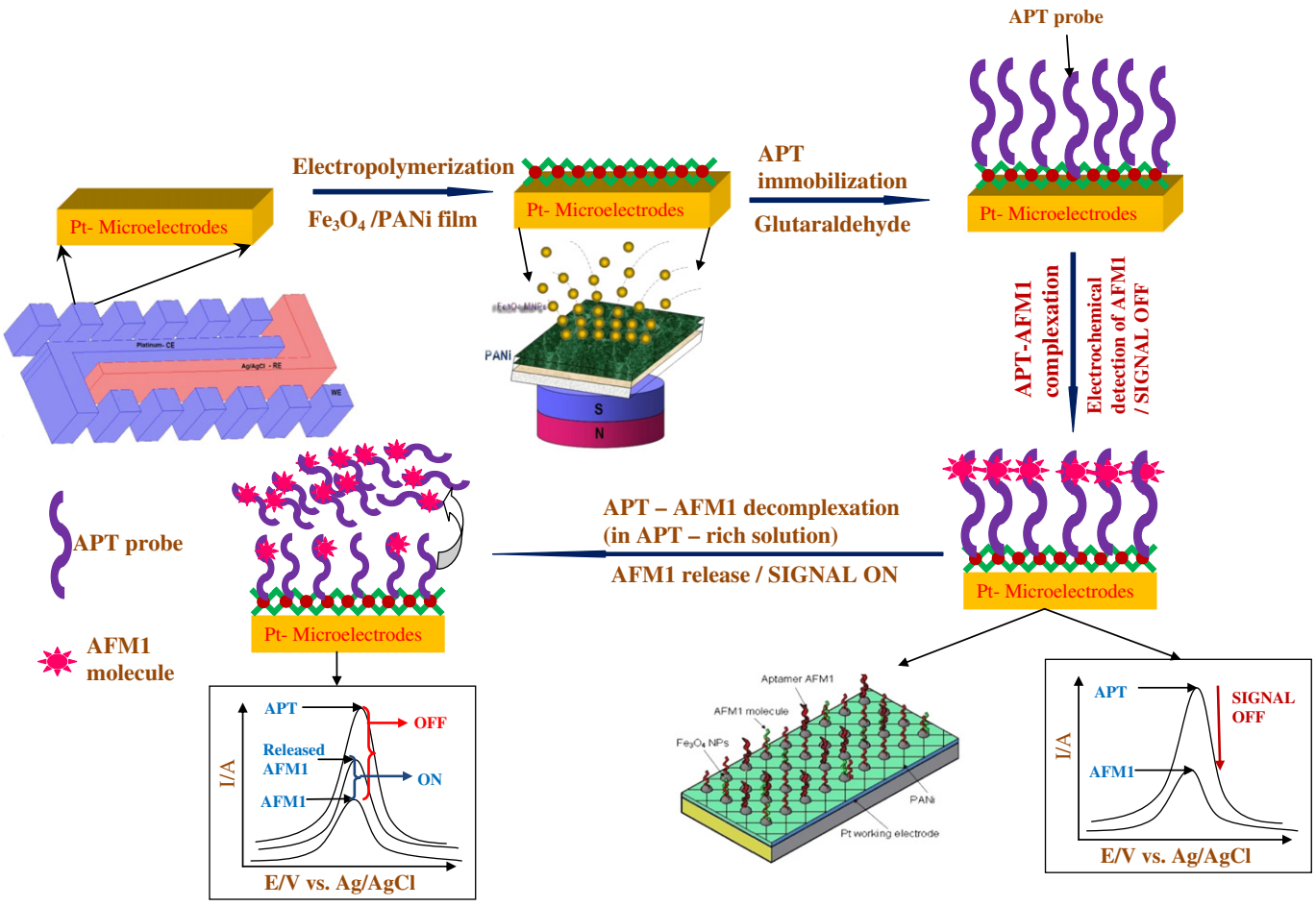

Fig. 3. Principle of label-free detection of AFM1 with magneto-electrochemical Fe_3O_4/PANi based aptasensor.

($R^2 = 0.9986$) in the range of 6–60 ng·L^{-1} with the limit of detection (LOD) of 1.98 ng·L^{-1}, respectively (inset of Fig. 5). The detailed procedure for LOD calculation was included in Supporting Information. To the best of our knowledge, the value of LOD (1.98 ng·L^{-1}), obtained in this study, is comparable to the best results, very recently reported in literature [32,35–46] (Table 1).

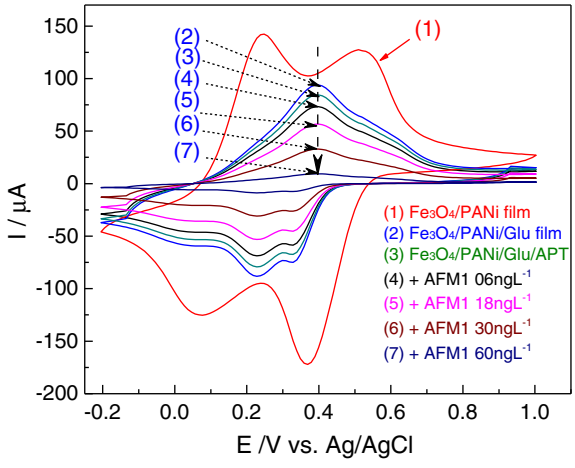

Fig. 4. SIGNAL OFF detection: CVs recorded during APT–AFM1 complexation with Fe_3O_4/PANi IDA recorded in HCl 0.1 M (curve 1); after treatment with Glutaraldehyde (curve 2), after immobilization with 180 pM APT (curve 3) and after complexation with 6–60 ng·L^{-1} AFM1(curves 4–7).

Taking into account the strong but reversible interaction between APT and AFM1, competitive reactions of AFM1 with tightly conjugated APT on solid electrode surface (on the one side) and free APT in solution (in much larger quantity and denser concentration, on the other side) should occur, by virtue of equilibrium displacement. Effectively, the treatment of IDA in APT-rich solution has "freed up" some AFM1 (from APT–AFM1 complexes) that leaves the electrode surface to go into the solution where APT concentration was much higher. This signal-on experiment (Fig. 6A), leading to SWV signal increase, is a

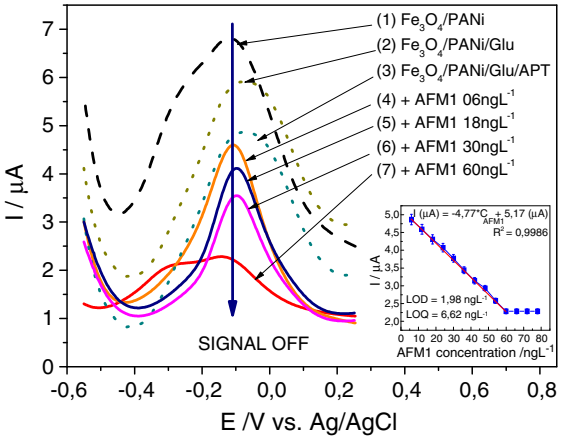

Fig. 5. SIGNAL OFF detection: SWVs recorded during APT–AFM1 complexation, carried out in the same conditions as described in Fig. 4 (inset: the response curve of the aptasensor with AFM1 concentration range from 6 to 80 ng·L^{-1}).

Table 1
Summary of recent publications relevant to the detection of Aflatoxin M1.

Reference	Analytical method	LOD	Linear range
[32]	CV	8 $ng \cdot L^{-1}$	10–100 $ng \cdot L^{-1}$
[35]	CV and EIS	0.4 $ng \cdot mL^{-1}$	1–14 $ng \cdot mL^{-1}$
[36]	Electrochemical immunoassay	25 $pg \cdot mL^{-1}$	30–240 $ng \cdot mL^{-1}$
[37]	ELISA	1 $pg \cdot mL^{-1}$	5–250 $pg \cdot mL^{-1}$
[38]	FI-IA with amperometric detection	11 ppt	20–500 ppt
[39]	ELISA	1 $ng \cdot L^{-1}$	2.5–80 $ng \cdot L^{-1}$
[40]	Immunoassay	0.025 $ng \cdot mL^{-1}$	0.05–1 $ng \cdot mL^{-1}$
[41]	SPFS	0.6 $pg \cdot mL$	1–100 $pg \cdot mL^{-1}$
[42]	SPR	3 $ng \cdot mL^{-1}$	–
[43]	Chemiluminescent immunoassay	0.25 $pg \cdot mL^{-1}$	–
[44]	Potentiometric immunosensor	40 $pg \cdot mL^{-1}$	125–2000 $pg \cdot mL^{-1}$
[45]	HPLC with post-column	1 $ng \cdot kg^{-1}$	–
[46]	Impedimetric immunosensor	1 $pg \cdot mL^{-1}$	6.25–100 $pg \cdot mL^{-1}$

Abbrevitations: Cyclic Voltammetry (CV), Electrochemical Impedance Spectroscopy (EIS), Enzyme-linked immunosorbent assay (ELISA), Flow-Injection Immunoassay (FI-IA), High-performance liquid chromatography (HPLC), surface plasmon-enhanced fluorescence spectroscopy (SPFS), and surface plasmon resonance (SPR).

very interesting feature of the above aptasensor, inferring that the signal-off trend when adding AFM1 really comes from true reversible complexation between APT and AFM1 but not any other interfering phenomena like non-specific adsorption or signal instability.

3.2. Reproducibility and stability

Another advantage of the above electrode was its working stability which was tested by measuring the voltammetric current decay during repetitive SWV cycling. It was found that the SWV peak height practically remains its initial value with a relative standard deviation (R.S.D.) less than 5% for 20 successive measurements, indicating an excellent reproducibility of above proposed modified electrode. Furthermore, it is possible to perform decomplexation followed by re-complexation and so on for at least 10 times, thus indicating the good reversibility of APT–AFM1 interaction as well as the robustness of this interdigitated electrode based arrays.

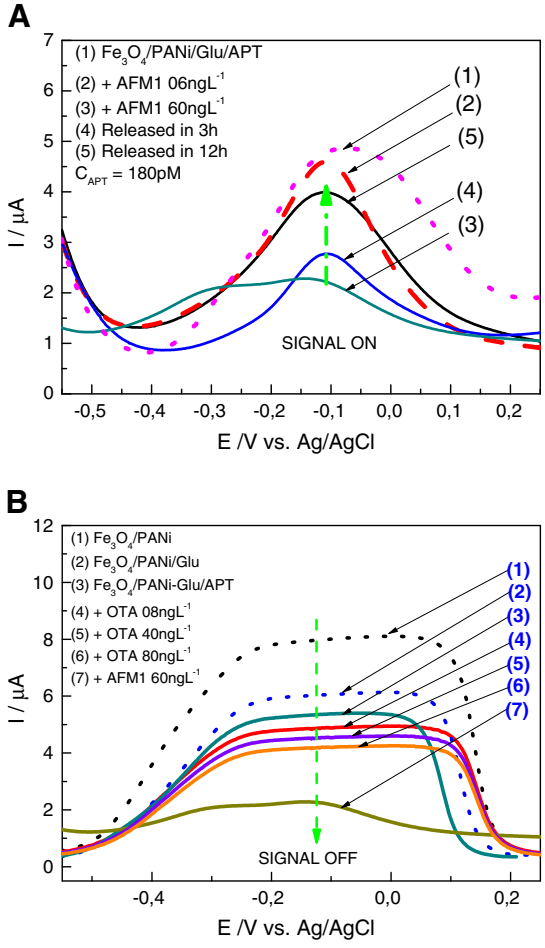

Fig. 6. A. SIGNAL ON detection: SWVs recorded during APT–AFM1 decomplexation after 3- and 12-hour release of AFM1 in APT rich solution. B. Selectivity experiment: SWVs recorded during complexation with irrelevant OTA.

3.3. Selectivity

Generally, antigen–antibody cross-reactivity (the ability of the combining site of an antibody to react with more than one antigen because of the similar antigenic structure, leading to false positive values), is an important parameter to evaluate selectivity. In our case, selectivity experiments were carried out with an irrelevant OTA (molecular weight is 428 Da, almost the same as AFM1). As shown in Fig. 6B, much less significant signal drop, acquired from cross-reactivity among AFM1/OTA was observed (due to cross-reaction between APT-OTA, much less OTA molecules were bound onto the surface of the aptasensor). It is the high specificity of the corresponding APT–AFM1 interaction that fulfills the main objective of this study. Further, to answer the question whether this aptasensor is suitable for quantifying the AFM1 concentration in real samples, cross-activity tests between APT and other toxins (B1, B2, M2, G1 and G2) should be carried out individually (although according to the literature, those cross-activity values are almost the same because they were from the same class (mycotoxin) with the same properties [47]). Moreover, some other critical issues such as i) evaluation of the sensor response in real complex matrix (serum or spiked milk matrix), ii) evaluation of long-term stability and reproducibility, and iii) the construction of micro-sensor array using the same analytical scheme for high throughput analysis should be investigated and reported in the following paper.

4. Conclusion

In this work, Fe_3O_4/PANi-based electrochemical aptasensor for AFM1 detection was developed and characterized. The use of magnetic nanoparticles is analytically attractive because of their signal amplification role. The developed aptasensor is able to detect AFM1 far below the legislative detection limit set. Our study demonstrates the viability of the aptasensor as a potential complementary strategy in the analysis of contaminated AFM1 in milks, providing advantages over other analytical techniques in terms of label free format, sensitivity, stability, analysis time and cost effectiveness. The further works are under progress for selectivity improvement of the aptasensor for real samples as well as for other pathogenic detection.

Acknowledgment

This work was supported by the Vietnam National Foundation for Science and Technology Development (NAFOSTED) grant No. 104.03-2010.60.

Appendix A. Supplementary data

Supplementary data to this article can be found online at http://dx.doi.org/10.1016/j.msec.2013.01.044.

References

[1] S.S. Deshpande, Handbook of Food Toxicology (Food Science and Technology), 1st ed. CRC Press, 2002.
[2] J. Shashidhar, R.B. Sashidhar, V. Deshpande, FEMS Microbiol. Lett. 251 (2005) 113–117.
[3] P.J. Cotty, R. Jaime-Garcia, Int. J. Food Microbiol. 119 (2007) 109–115.
[4] J. Fink-Gremmels, Food Addit. Contam. Part A 25 (2008) 172–180.
[5] P. Li, Q. Zhang, W. Zhang, TrAC Trends Anal. Chem. 28 (2009) 1115–1126.
[6] H.S. El-Nezami, G. Nicoletti, G.E. Neal, D.C. Donohue, J.T. Ahokas, Food Chem. Toxicol. 33 (1995) 173–179.
[7] E.K. Kim, D.H. Shon, D. Ryu, J.W. Park, H.J. Hwang, Y.B. Kim, Food Addit. Contam. 17 (2000) 59–64.
[8] K. Thirumala-Devi, M.A. Mayo, A.J. Hall, P.Q. Craufurd, T.R. Wheeler, F. Waliyar, A. Subrahmanyam, D.V.R. Reddy, J. Agric. Food Chem. 50 (2002) 933–937.
[9] C.E. López, L.L. Ramos, S.S. Ramadán, L.C. Bulacio, Food Control 14 (2003) 31–34.
[10] M.L.R. Velasco, M.M.C. Delso, D.O. Escudero, Food Addit. Contam. 20 (2003) 276–280.
[11] S. Rastogi, P.D. Dwivedi, S.K. Khanna, M. Das, Food Control 15 (2004) 287–290.
[12] B. Sarımehmetoglu, O. Kuplulu, T. Haluk Celik, Food Control 15 (2004) 45–49.
[13] A. Logrieco, D.W.M. Arrigan, K. Brengel-Pesce, P. Siciliano, I. Tothill, Food Addit. Contam. 22 (2005) 335–344.
[14] A. Radoi, M. Targa, B. Prieto-Simon, J.L. Marty, Talanta 77 (2008) 138–143.
[15] K. Helrich, Official methods of analysis of the Association of Official Analytical Chemists (AOAC), Arlington, 1990.
[16] E.W. Sydenham, G.S. Shephard, Progress in Food Contaminant Analysis, Blackie Academic and Professional, London, 1996.
[17] L. Lin, J. Zhang, P. Wang, Y. Wang, J. Chen, J. Chromatogr. A 815 (1998) 3–20.
[18] A. Kamkar, Food Control 17 (2006) 768–775.
[19] R.J. Cole, Modern Methods in the Analysis and Structural Elucidation of Mycotoxins, 1st ed. Academic Pr, 1986.
[20] S. Dragacci, F. Grosso, J. Gilbert, J. AOAC Int. 84 (2) (March 2001) 437–443.
[21] M. Bognanno, L. La Fauci, A. Ritieni, A. Tafuri, A. De Lorenzo, P. Micari, L. Di Renzo, S. Ciappellano, V. Sarullo, F. Galvano, Mol. Nutr. Food Res. 50 (2006) 300–305.
[22] M. Wojciechowski, R. Sundseth, M. Moreno, R. Henkens, Clin. Chem. 45 (1999) 1690–1693.
[23] S. Piermarini, L. Micheli, N.H.S. Ammida, G. Palleschi, D. Moscone, Biosens. Bioelectron. 22 (2007) 1434–1440.
[24] A.D. Ellington, J.W. Szostak, Nature 346 (1990) 818–822.
[25] C. Tuerk, L. Gold, Science 249 (1990) 505–510.
[26] S.D. Jayasena, Clin. Chem. 45 (1999) 1628–1650.
[27] D.J. Patel, A.K. Suri, Rev. Mol. Biotechnol. 74 (2000) 39–60.
[28] K. You, S. Lee, A. Im, S. Lee, Biotechnol. Bioprocess Eng. 8 (2003) 64–75.
[29] I. Willner, M. Zayats, Angew. Chem. Int. Ed. 46 (2007) 6408–6418.
[30] R. Stoltenburg, C. Reinemann, B. Strehlitz, Biomol. Eng. 24 (2007) 381–403.
[31] M. Velasco-Garcia, S. Missailidis, Gene Ther. Mol. Biol. 13 (2009) 1–10.
[32] C.O. Parker, Y.H. Lanyon, M. Manning, D.W. Arrigan, I.E. Tothill, Anal. Chem. 81 (2009) 5291–5298.
[33] T.T. Luong, T.P. Ha, L.D. Tran, M.H. Do, T.T. Mai, N.H. Pham, H.B.T. Phan, G.H.T. Pham, N.M.T. Hoang, Q.T. Nguyen, P.X. Nguyen, Colloids Surf., A Physicochem. Eng. Asp. 384 (2011) 23–30.
[34] A.J. Bard, L.R. Faulkner, Electrochemical Methods: Fundamentals and Applications, 2nd ed. Wiley, 2000.
[35] E. Dinçkaya, Ö. Kınık, M.K. Sezgintürk, Ç. Altuğ, A. Akkoca, Biosens. Bioelectron. 26 (2011) 3806–3811.
[36] L. Micheli, R. Grecco, M. Badea, D. Moscone, G. Palleschi, Biosens. Bioelectron. 21 (2005) 588–596.
[37] D. Neagu, S. Perrino, L. Micheli, G. Palleschi, D. Moscone, Int. Dairy J. 19 (2009) 753–758.
[38] M. Badea, L. Micheli, M.C. Messia, T. Candigliota, E. Marconi, T. Mottram, M. Velasco-Garcia, D. Moscone, G. Palleschi, Anal. Chim. Acta 520 (2004) 141–148.
[39] P. Rosi, A. Borsari, G. Lasi, S. Lodi, A. Galanti, A. Fava, S. Girotti, E. Ferri, Int. Dairy J. 17 (2007) 429–435.
[40] L. Sibanda, S. De Saeger, C. Van Peteghem, Int. J. Food Microbiol. 48 (1999) 203–209.
[41] Y. Wang, J. Dostálek, W. Knoll, Biosens. Bioelectron. 24 (2009) 2264–2267.
[42] S.J. Daly, G.J. Keating, P.P. Dillon, B.M. Manning, R. O'Kennedy, H.A. Lee, M.R.A. Morgan, J. Agric. Food Chem. 48 (2000) 5097–5104.
[43] M. Magliulo, M. Mirasoli, P. Simoni, R. Lelli, O. Portanti, A. Roda, J. Agric. Food Chem. 53 (2005) 3300–3305.
[44] S. Rameil, P. Schubert, P. Grundmann, R. Dietrich, E. Märtlbauer, Anal. Chim. Acta 661 (2010) 122–127.
[45] A.C. Manetta, L. Di Giuseppe, M. Giammarco, I. Fusaro, A. Simonella, A. Gramenzi, A. Formigoni, J. Chromatogr. A 1083 (2005) 219–222.
[46] G. Bacher, S. Pal, L. Kanungo, S. Bhand, Sensors Actuators B Chem. 168 (2012) 223–230.
[47] Ying Wang, Nan Liub, Baoan Ning, Ming Liu, Zhiqiang Lv, Zhiyong Sun, Yuan Peng, Cuicui Chen, Junwen Li, Zhixian Gao, Biosens. Bioelectron. 34 (1) (2012) 44–50.